

# Closing the Loop: A High-Performance Connectivity Solution for Realizing Wireless Closed-Loop Control in Industrial IoT Applications

Adnan Aijaz, *Senior Member, IEEE*, and Aleksandar Stanoev

**Abstract**—High-performance real-time wireless connectivity is at the heart of the Industrial Internet-of-Things (IIoT). Realizing wireless closed-loop control is crucial for various mission-critical IIoT systems. Existing wireless technologies fall short of meeting the stringent performance requirements of closed-loop control. This paper presents a novel wireless solution, called **GALLOP**, for realizing closed-loop control over multi-hop or single-hop networks. **GALLOP** adopts a pragmatic design approach for addressing the challenges of wireless closed-loop control. Key design aspects of **GALLOP** include control-aware bi-directional scheduling for cyclic exchange, robust retransmission techniques based on cooperative multi-user diversity and low-overhead signaling for scalable operation. **GALLOP** has been specifically designed for control loops that are closed over the whole network with dynamics on the order of few milliseconds. Performance evaluation based on extensive system-level simulations and hardware implementation on a Bluetooth 5 testbed demonstrates that **GALLOP** provides high-performance connectivity with very low and deterministic latency, very high reliability and high scalability, to meet the stringent requirements of wireless closed-loop control for versatile IIoT applications.

**Index Terms**—Closed-loop, cooperative, cyber-physical systems, distributed, industrial wireless, IIoT, multi-hop, networked control system, real-time, scheduling, wireless control.

## I. INTRODUCTION

THE recent *Industrial Internet-of-Things* (IIoT) [2] initiative is broadly focusing on application of connectivity technologies in industrial domains such as manufacturing, transportation, logistics, and energy. Unlike consumer IoT systems, IIoT systems focus on connecting industrial assets like machines and control systems with information technologies and business processes [3], [4]. IIoT systems are mission-critical in nature and require high-performance connectivity to fulfil the stringent requirements of timeliness and reliability [5].

Closed-loop control or feedback control is a prominent industrial control application. Typically, it takes place between a controller and a spatially distributed system of sensors and actuators. Control and feedback signals are exchanged in the form of information packets over a shared wireless medium, thereby closing a global control loop. In legacy industrial systems, closed-loop control is realized through wired technologies like Industrial Ethernet [6]. However, such technologies have high installation and maintenance costs. Multi-hop wireless communication based on low-power wireless devices

provides a cost-effective and flexible connectivity solution. However, state-of-the-art multi-hop wireless technologies like WirelessHART, ZigBee and ISA 100.11a do not fulfil the challenging connectivity requirements of industrial closed-loop control applications. Such technologies are mainly used for non-critical applications like monitoring of large-scale industrial systems.

Designing a multi-hop wireless network for closed-loop control becomes particularly challenging due to its stringent connectivity requirements. Closed-loop control has strong real-time requirements and demands connectivity with very high reliability and very low latency [7]. This is because packet losses and delays, which are dominant in wireless environments, have a detrimental effect on the stability of control loops. Closed-loop control involves bi-directional communication with cyclic traffic patterns. The cyclic information exchange demands highly deterministic connectivity which implies that the communication latency (between cycles) must have a very low variance. The presence of a large number of sensors and actuators also creates the requirement of highly scalable connectivity.

Against this background, the objective of this paper is to design a high-performance connectivity solution for realizing wireless closed-loop control over multi-hop networks. Our focus is specifically on *wireless design for control loops that are closed over the entire multi-hop network with dynamics on the order of few milliseconds (ms)*. We propose a novel wireless solution, termed as **GALLOP** (GenerAlized cLosed-Loop cOntrol of Processes) that has been designed to address the challenges of multi-hop closed-loop control. Although **GALLOP** has been designed for multi-hop networks, it is fully capable of operating in single-hop scenarios. **GALLOP** design encompasses various novel features (Section III-A), which provide high-performance wireless connectivity with very low and deterministic latency, very high reliability and high scalability. **GALLOP** can be extended to a broad range of IIoT applications. The key contributions of this work are summarized as follows.

- **GALLOP** handles cyclic information exchange through multi-hop time division multiple access (TDMA) scheduling. We design a novel *distributed* multi-hop scheduling algorithm for **GALLOP** which is described in Section III.
- We design novel techniques for handling medium access control (MAC) layer transmission failures in **GALLOP**. These techniques, which are discussed in Section IV, ensure reliable operation in harsh wireless environments.

The authors are with Toshiba Europe Ltd., Bristol, BS1 4ND, U.K. Contact e-mail: adnan.aijaz@toshiba-bril.com

Part of this work has been presented at the 27th International Conference on Real-Time Networks and Systems (RTNS), 2019 [1].

- We develop an analytic framework (Section V) for characterizing convergence aspects of distributed scheduling.
- We conduct a comprehensive evaluation of GALLOP through system-level simulations (Section VI).
- We provide experimental results (Section VII) for GALLOP based on hardware implementation on a state-of-the-art Bluetooth 5 platform and evaluation on a real Bluetooth 5 testbed. We also benchmark the performance against a standard solution.

An early version of this work appeared in [1]. This paper provides a number of new contributions including extensions to protocol design, analysis of convergence time and further evaluation based on system-level simulations and hardware implementation.

## II. RELATED WORK

The problem of wireless closed-loop control can be approached from two different perspectives: *control-aware wireless design* and *wireless-aware control design*. The control-aware wireless design paradigm, which is the focus of this work, aims to design network protocols for meeting the stringent connectivity requirements of control-centric applications. Existing solutions for control-aware wireless are mainly focused on single-hop connectivity. Wireless Interface for Sensors and Actuators (WISA) [8] is one of the earliest solutions designed for industrial automation networks. The Wireless Sensor Actuator Network for Factory Automation (WSAN-FA) standard [9] adopted WISA with certain modifications. WISA as well as WSAN-FA target a latency of 10 ms for up to 120 devices. However, both solutions offer insufficient reliability for the target latency performance. Both WISA and WSAN-FA have also influenced the development of the recent IO-Link Wireless standard [10] which targets a latency of 5 ms for up to 40 devices in single-hop. Through novel enhancements and optimizations, ENCLOSE [11] outperforms WISA, WSAN-FA and other similar industrial wireless solutions in terms of reliability, latency, scalability, and coverage. Control-centric wireless solutions based IEEE 802.11 standard (Wi-Fi) have also been developed. Prominent solutions include Industrial Wireless Local Area Network (IWLAN) [12] and Wireless Network for Industrial Automation - Factory Automation (WIA-FA) [13]. The latest IEEE 802.11ax standard is particularly attractive for industrial wireless applications as it provides much lower latency compared to previous Wi-Fi generations [14]. EchoRing [15] achieves highly reliable and responsive connectivity based on a token-passing algorithm. Even though it extends beyond single-hop connectivity, it is not as scalable as WISA and WSAN-FA. The 5G mobile/cellular technology is also a candidate for control-centric industrial applications [16], [17].

On the contrary, the objective of the wireless-aware control design paradigm is to develop control algorithms to cope with wireless imperfections. Alur *et al.* [18] developed a compositional framework for modeling and analysis of multi-hop control networks. The framework separates control, topology, routing, and scheduling aspects and allows co-design of control algorithms and communication parameters. Smarra *et*

*al.* [19] addressed the problem of guaranteed stability with co-design of a digital controller and network parameters. Pajic *et al.* [20] proposed a new approach that treats the multi-hop network as a controller. Tatikonda and Mitter [21] investigated bounds on required channel rates to achieve different control objectives. Robinson and Kumar [22] investigated the problem of minimizing packet drops through optimization of controller location. Zhang *et al.* [23] surveyed different control methodologies for tackling network-induced imperfections.

Multi-hop TDMA scheduling in wireless networks has been extensively surveyed in a recent study [24]. Multi-hop scheduling in GALLOP is unique in various aspects. First, it has been designed for closed-loop control that entails bi-directional exchange, which has been rarely considered in prior art, particularly in the case of distributed techniques. Second, distributed scheduling in GALLOP adopts a pragmatic approach and implements a novel signaling mechanism. Existing scheduling techniques seldom consider such practical aspects. Third, scheduling in GALLOP is particularly optimized to minimize cyclic latency. Fourth, scheduling in GALLOP provides native support for cooperative transmissions that are crucial for high reliability. Last, but not least, scheduling in GALLOP handles MAC layer transmission failures while accounting for the peculiarities of closed-loop control.

## III. GALLOP – DESIGN AND PROTOCOL OPERATION

### A. Key Aspects

GALLOP has been designed for high-performance wireless connectivity in order to realize closed-loop control over multi-hop networks. The centerpiece of GALLOP design is a *control-aware bi-directional schedule* that handles cyclic exchange of control information between a controller and a spatially distributed system of sensors and actuators. To reduce cycle time, the scheduling algorithm exploits both parallel and sequential transmissions for minimizing the cycle time which is a key metric for closed-loop control. GALLOP builds a distributed schedule through a *low-overhead signaling* approach that exploits local overhearing. To achieve fast convergence, signaling is performed jointly for both downlink and uplink. GALLOP implements *robust and efficient retransmission techniques* that ensure high reliability. Some of its retransmission techniques harness *cooperative multi-user diversity* by integrating cooperative and multi-user diversity techniques. The retransmission techniques also exploit opportunities for network coding that provides low latency and high reliability. GALLOP also supports *frequency/channel hopping* for mitigating the impact of external interference. The design of GALLOP is agnostic to the Physical (PHY) layer. Our implementation is based on the Bluetooth PHY layers. However, it can be implemented on any other PHY layer (IEEE 802.15.4, IEEE 802.11, etc.).

### B. Scenario, Assumptions and PHY/MAC Layer Design

We consider a closed-loop control scenario which is shown in Fig. 1. Multiple devices (sensors, actuators, etc.) exchange bi-directional and cyclic information with a controller over a multi-hop or a single-hop wireless network. This scenario

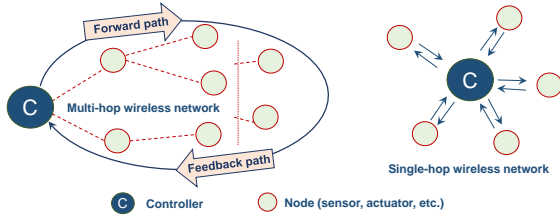


Fig. 1. Multi-hop and single-hop control scenarios for GALLOP.

reflects a broad range of mission-critical IIoT applications. Some of the key applications are described as follows.

- In industrial automation, cyclic exchange of command and feedback messages occurs between a controller and multiple robotic arms.
- In case of vehicle platooning, a lead vehicle (controller) maintains constant velocity/distance for the followers through closed-loop interaction. Similar principle can be applied to leader-follower formation control [25] of automated guided vehicles in logistics and warehouse operations.
- In a large-scale battery network, a battery management unit (controller) monitors and controls individual battery cells through cyclic exchange of command and feedback messages.

For protocol operation, the terms *downlink* and *uplink* refer to communication from the controller to nodes/devices and vice versa, respectively. Without any network layer protocol, the nodes constitute a mesh topology. We assume that the mesh topology has been converted into a tree topology through any low-cost routing protocol (e.g., RPL [26]). The tree topology provides multi-hop connectivity between the controller and the devices. We consider a simple interference model where two nodes are one-hop neighbors if their mutual distance is less than the communication or interference range. For achieving network-wide time synchronization, GALLOP utilizes a flooding-based protocol, known as Glossy [27]. The flooding process is initiated by the controller and driven by radio events. It exploits synchronous/concurrent transmissions and entails relaying overheard packets immediately upon reception. Time synchronization based on Glossy has been described in detail in [27]. It is emphasized that other time synchronization techniques can also be adopted for GALLOP implementation.

Our implementation of GALLOP is based on the PHY layer of Bluetooth technology which is quite promising for industrial communication [7]. Although GALLOP can be realized on both basic rate (BR) and low energy (LE) Bluetooth radios, our implementation is on the latter. The LE radio provides a data rate of 1 Mbps (referred to as LE 1M PHY). The latest Bluetooth 5 standard introduces two new PHY layers: LE 2M PHY which supports a data rate of 2 Mbps, and LE Coded PHY that supports a data rate of 500kbps or 125 kbps. The MAC layer of GALLOP is based on the principles of multi-hop TDMA and frequency division duplexing (FDD). There are three different MAC frames: a downlink frame for downlink communication, an uplink frame for uplink communication and a signaling frame for exchange of schedule-related information. Each frame comprises a certain number

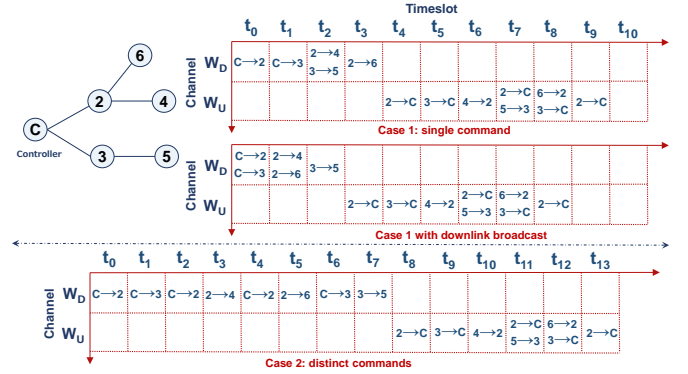


Fig. 2. Centralized bi-directional multi-hop scheduling in GALLOP. of timeslots of fixed duration.

### C. Centralized Bi-directional Multi-hop Scheduling

To elaborate on the scheduling problem for multi-hop wireless closed-loop control, we discuss a centralized solution where the controller is responsible for deriving a schedule based on global knowledge of network topology. We consider the topology in Fig. 2 where the connectivity (neighborhood) information at the MAC layer for each node is as follows.

$$\begin{cases} C : [2, 3], & \text{node 2} : [C, 4, 6], & \text{node 3} : [C, 5], \\ \text{node 4} : [2, 6], & \text{node 5} : [3], & \text{node 6} : [2, 4] \end{cases} \quad (1)$$

The controller's objective is to minimize *cycle time* which is defined as the cumulative time of successfully transmitting command messages to all the nodes in the network and successfully receiving the response message from each node. We consider the case where the controller transmits a single command message for the network. The controller implements a simple scheduling algorithm where downlink and uplink transmissions are scheduled in a sequential manner while exploiting parallel transmission opportunities. The constructed schedule is shown in Fig. 2. First, the controller sequentially schedules downlink transmissions (command messages) on a downlink channel  $W_D$ . The downlink transmissions from nodes 2 and 3 are non-conflicting; hence, these can go in parallel. After downlink scheduling, which takes 4 timeslots, the controller initiates uplink scheduling on the uplink channel  $W_U$ . Non-conflicting uplink transmissions are scheduled in parallel. The overall cycle time is 10 timeslots. Note that the controller can also schedule downlink transmissions in a broadcast manner as illustrated in Fig. 2. This decreases the cycle time by a timeslot. The scheduling for distinct command messages (also shown in Fig. 2) for each node follows a similar approach with the exception of scheduling distinct downlink transmissions.

Due to the overhead of acquiring topological information and schedule dissemination, centralized scheduling techniques offer limited scalability. Therefore, the main focus of this work is distributed scheduling.

### D. Distributed Bi-directional Multi-hop Scheduling

In the distributed case, there is neither a central entity nor global knowledge of network topology. Schedule synthesis occurs via neighbor-to-neighbor information exchange

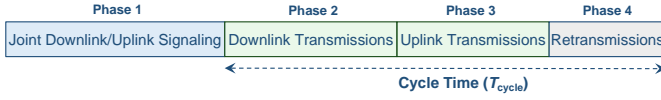


Fig. 3. Different phases of GALLOP protocol operation.

and negotiation. The fundamental principle of GALLOP's distributed scheduling is to construct a conflict-free schedule through parent-child handshake and local overhearing. Such information exchange occurs over a signaling frame (signaling channel). GALLOP implements different types of signaling messages. The *request-for-slots* (RFS) message is used by a child node to request resources (e.g., timeslots) from its parent node. Different RFS messages are employed in downlink and uplink, i.e., RFS-Downlink (RFS-D) and RFS-Uplink (RFS-U), respectively. In response to the RFS message, a parent node uses an *assignment* (ASGN) message to allocate resources to a child node. The *downlink signaling* (DLS) message is used by a parent node to disseminate schedule-related information to its child nodes. The signaling frame contains three different types of signaling slots. The first slot ( $s_0$ ) is a DLS slot and reserved for the controller. This is followed by a repetitive pattern (illustrated in Fig. 4) of three slots such that the RFS slots, the ASGN slots and the DLS slots are indexed by  $\{s_1, s_4, s_7, \dots\}$ ,  $\{s_2, s_5, s_8, \dots\}$  and  $\{s_3, s_6, s_9, \dots\}$ , respectively.

Fig. 3 shows different phases of GALLOP operation. The first phase is joint downlink/uplink signaling where schedules for downlink and uplink transmissions are built. An alternate approach is to decouple the signaling such that it occurs separately for downlink and uplink schedules. However, our experience of hardware implementation (discussed later) reveals that joint downlink/uplink signaling not only decreases the signaling phase duration but also reduces the cycle time.

Let  $\mathcal{M} = \{1, 2, \dots, M\}$  denote the set of nodes of the multi-hop network. The set of parent nodes and leaf nodes that constitute the network is denoted by  $\mathcal{R}$  and  $\mathcal{F}$ , respectively. A parent node has at least one child node associated with it at the network layer. The leaf nodes in the network are those with no child nodes. We assume that each parent node knows the number of its child nodes based on the information from the network layer.

GALLOP builds a sequential schedule in order to minimize the latency for cyclic information exchange. This implies that, in the downlink, the schedule begins from the controller and evolves towards the leaf nodes. Similarly, in the uplink it begins from the leaf nodes and evolves towards the controller. Sequential scheduling becomes feasible due to the unique signaling mechanism of GALLOP. Nodes maintain *local knowledge* of available timeslots and channels through overhearing of different signaling messages during the signaling phase. The distributed scheduling process exploits local knowledge and follows a set of policies and rules that dictate schedule construction.

**Policy for Downlink Signaling** – This policy dictates access to the signaling channel and plays an important role in overall schedule construction. It consists of a single rule.

**Rule DL-1:** Any parent node  $r \in \mathcal{R}$  assigns priorities to

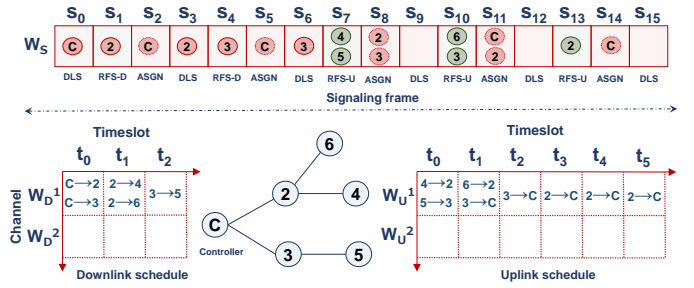


Fig. 4. Distributed bi-directional multi-hop scheduling in GALLOP.

its child nodes and conveys the information regarding next available RFS slot using the DLS message.

The priority of a node can be based on any unique parameter such as its rank at the network-layer or its MAC identifier. The prioritization of child nodes in any order does not affect the schedule building process. The child nodes use the priority information for conflict-free access to the signaling frame.

**Policy for Parent-Child Handshake** – The objective of this policy is conflict-free resource allocation in the multi-hop network. It is based on three different rules.

**Rule H-1:** Any child node  $m \in \mathcal{M}$  requests the earliest possible timeslots on a given channel through the RFS message where it finds no conflict as per its local knowledge.

**Rule H-2:** Upon reception of an RFS message, any parent node  $r \in \mathcal{R}$  confirms the requested allocation by transmitting an ASGN message if it finds no conflict based on its local knowledge.

**Rule H-3:** If a parent node  $r \in \mathcal{R}$  detects a conflict in requested allocation, it responds with an updated allocation, in the ASGN message, as per its local knowledge of earliest available timeslots on a given channel.

We explain the role of these two policies in building the downlink schedule through the topology shown in Fig. 4 that has the same MAC layer neighborhood/connectivity relationship as given by (1). The signaling process is initiated by the controller through transmission of a DLS message in the first signaling slot ( $s_0$ ) of the signaling channel  $W_S$ . As per the policy for downlink signaling, it assigns priorities to its child nodes (nodes 2 and 3). We assume that a lower node ID<sup>1</sup> corresponds to a higher priority. Therefore, node 2 has priority over node 3. The DLS message from the controller also contains the index of the next available RFS slot (denoted by  $ix\_RFS\_slot$ ), i.e.,  $s_1$ . Any child node computes the index of its RFS slot as  $ix\_RFS\_slot + priority - 1$ . Since node 2 has the highest priority, it determines its RFS slot as  $s_1$ . Node 3 determines its RFS slot as  $s_4$ , as it has the second priority. Note that the controller is exempt from handshake. In the downlink, the controller (and any other parent node) can either schedule its child nodes in a unicast (distinct timeslots) or a broadcast (single timeslot) manner. We focus on the latter case as the former is straightforward extension of the proposed mechanism. For downlink transmission, the controller selects timeslot  $t_0$  on the downlink channel  $W_D$ . The schedule information of the controller is also included

<sup>1</sup>A parent node knows the node IDs of its child nodes from the network setup phase when the routing tree is generated.



in the DLS message. In case of distinct transmissions, the controller would have selected timeslots  $t_0$  and  $t_1$ . As per node 2's local knowledge, timeslot  $t_0$  is not available. Hence, based on Rule H-1, it picks timeslot  $t_1$  and transmits an RFS-D message in slot  $s_1$ . As the controller does not detect a conflict, it confirms the allocation as per Rule H-2 by transmitting an ASGN message in the next ASGN slot  $s_2$ . After successful downlink allocation, any parent node uses the first available DLS slot to transmit the DLS message as per the policy for downlink signaling. Hence, node 2 selects slot  $s_3$  to transmit a DLS message to its child nodes (nodes 4 and 6). The DLS message also contains the index of the next available RFS slot. Node 2 has the information regarding the number of child nodes of the controller (based on the received DLS message). It determines that the first two RFS slots would be taken by the child nodes of the controller. Therefore, the next available RFS slot for its child nodes is  $s_7$ . In slot  $s_4$ , node 3 sends an RFS-D message to the controller. Nodes 2 and 3 are not in the neighborhood of each other. We assume that the ASGN message in slot  $s_2$  (from the controller) was not successfully overheard by node 3. Hence, as per Rule H-1, node 3 requests timeslot  $t_1$  on the downlink channel  $W_D$  from the controller. However, based on controller's local knowledge, this timeslot is taken by node 2. Therefore, as per Rule H-3, the controller allocates timeslot  $t_2$  through the ASGN message in slot  $s_5$ . After successful downlink allocation, node 3 uses the next available DLS slot, i.e., slot  $s_6$  to transmit a DLS message to node 5. Based on the local knowledge of node 3, the next available RFS slot for node 5 is  $s_7$ . This completes successful construction of the downlink schedule as all parent nodes have timeslots allocated for downlink transmissions.

In GALLOP, the uplink schedule construction process is initiated by the leaf nodes. Owing to joint downlink/uplink signaling, leaf nodes trigger uplink signaling (for schedule construction) that follows a set of policies and rules.

**Policy for Uplink Signaling** – This policy dictates access to the signaling channel for construction of the uplink schedule. It consists of the following rules.

**Rule UL-1:** Any parent node  $r \in \mathcal{R}$  ( $r \neq$  controller) requests uplink timeslots only if it has scheduled all of its child nodes in the uplink.

**Rule UL-2:** Any parent node  $r \in \mathcal{R}$  ( $r \neq$  controller) requests  $S_r + 1$  timeslots in the uplink, where  $S_r$  is the total number of timeslots requested by its child nodes.

Building a sequential schedule in uplink is a key aspect of the uplink signaling policy. Based on the DLS message from node 2, nodes 4 and 6 determine  $s_7$  and  $s_{10}$  as their RFS slots, respectively. Similarly, node 5 determines its RFS slot as  $s_7$  based on node 3's DLS message. Nodes 4 and 5 trigger the uplink schedule construction process in slot  $s_7$  as these are leaf nodes. As per Rule H-1, both nodes select timeslot  $t_0$  on the uplink channel  $W_U$  and transmit an RFS-U message to their parent nodes. Note that neither node 2 can overhear node 5 nor node 3 can overhear node 4, as they are not in the neighborhood of each other. Therefore, both nodes 4 and 5 can share the respective RFS slot without causing collisions at the respective receivers. As per Rule H-2, nodes 2 and 3 confirm the requested allocation through ASGN messages in slot  $s_8$ .

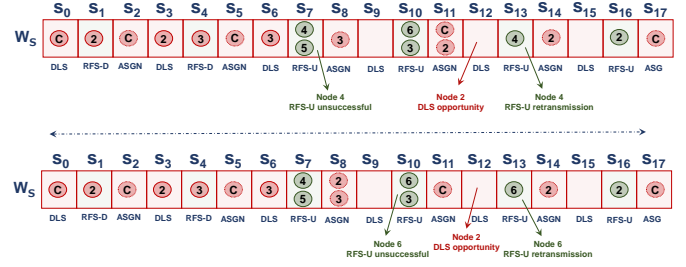


Fig. 5. Illustration of the signaling message retransmission policy. The topology is same as in Fig. 4.

Based on node 6's local knowledge, timeslot  $t_0$  is occupied. Hence, it selects timeslot  $t_1$  and transmits an RFS-U message in slot  $s_{10}$ . As per Rule H-2, Node 2 confirms the requested allocation by transmitting an ASGN message in slot  $s_{11}$ .

After successful allocation to node 5 in slot  $s_8$ , node 3 can now request timeslots for uplink communication as per Rule UL-1. Based on its local knowledge, the next available RFS slot is  $s_{10}$ . As per Rule UL-2, it requests two timeslots in an RFS-U message, i.e.,  $t_1$  and  $t_2$  on the uplink channel  $W_U$ . The controller confirms the requested allocation via an ASGN message in slot  $s_{11}$ . Node 2 is ready to request uplink timeslots after scheduling its child nodes. Based on its local knowledge, the next available RFS slot is  $s_{13}$ . Note that node 2 is not aware of the allocation for node 3. Since it requires three timeslots ( $S_2 = 2$ ), it requests  $t_2$ ,  $t_3$  and  $t_4$  on the uplink channel  $W_U$  via an RFS-U message. As the controller detects a conflict on timeslot  $t_2$  that has been allocated to node 3, it responds with an updated allocation, i.e., timeslots  $t_3 - t_5$  on the uplink channel  $W_U$ , via an ASGN message in slot  $s_{14}$ . This completes the uplink scheduling as all nodes have timeslots allocated for uplink transmissions.

**Policy for Signaling Message Retransmission** – This policy dictates access to the signaling frame in case of signaling message retransmissions. During the schedule construction phase, RFS and DLS messages are retransmitted under the following conditions.

- Any node  $m \in \mathcal{M}$  ( $m \neq$  controller) retransmits an RFS message if it does not receive an ASGN message from its parent node. This happens due to a collision in an RFS slot or a link-level RFS/ASGN transmission failure.
- Any parent node  $r \in \mathcal{R}$  retransmits a DLS message if it does not receive an RFS message from at least one of its child nodes within the *allocation window*, which is given by  $ix\_RFS\_slot + 3 \times \Theta_r - 1$ , where  $\Theta_r$  is the number of child nodes and  $ix\_RFS\_slot$  is the index of the RFS slot as advertised in the original DLS message.

The policy for signaling message retransmission consists of the following rules.

**Rule SR-1:** Any node  $m \in \mathcal{M}$  ( $m \neq$  controller) retransmits the RFS message (on first attempt) in an RFS slot whose index is determined as  $ix\_RFS\_slot + \Theta_r + priority - 1 - U_r$ , where  $\Theta_r$  and  $U_r$  denote the number of child nodes and the number of successfully allocated child nodes of its parent node  $r$ , respectively.

**Rule SR-2:** Any node  $m \in \mathcal{M}$  ( $m \neq$  controller) retransmits the RFS message (on second or higher attempt) in an RFS slot

whose index is determined as  $ix\_prev\_RFS\_slot + B_m + priority - 1$ , where  $ix\_prev\_RFS\_slot$  is the index of the last used RFS slot and  $B_m$  denotes a small random backoff that is uniformly distributed in the interval  $[1, 2, \dots, \Psi]$ .

Rule SR-1 ensures that an RFS retransmission does not disrupt the handshake process of a sibling node, i.e., a node having the same parent. It also ensures that a node does not have to wait for an arbitrary long duration before retransmitting an RFS message by accounting for the number of successfully allocated sibling nodes. This information is acquired through retransmitted DLS messages. Moreover, Rule SR-2 potentially avoids conflicts between multiple nodes in neighborhood of each other that require RFS retransmissions.

**Rule SR-3:** Any parent node  $r \in \mathcal{R}$  retransmits the DLS message if an opportunity for retransmission arises within the allocation window. Otherwise, on first attempt, it retransmits the DLS message in the first available DLS slot as per its local knowledge, and on second or higher attempt, in a DLS slot whose index is given by  $ix\_prev\_DLS\_slot + B_m - 1$ , where  $ix\_prev\_DLS\_slot$  is the index of the last used DLS slot and  $B_m$  denotes a small random backoff that is uniformly distributed in the interval  $[1, 2, \dots, \Psi]$ .

Note that the leaf nodes do not transmit DLS messages. Therefore, after a parent node has ascertained the need for DLS retransmission, a retransmission opportunity arises if any of its child nodes transmits an RFS-U message during the allocation window. An opportunity also arises if a parent node does not receive an RFS message from a child node in its assigned slot. Rule SR-3 ensures that a child node awaiting DLS for requesting resources does not have to wait for an arbitrary long duration while mitigating contention between multiple parent nodes requiring DLS retransmissions in neighborhood. A parent node embeds information of the number of successfully allocated child nodes in the retransmitted DLS message. This is used by a child node to compute appropriate RFS slot for retransmission as per Rule SR-1.

The retransmission procedure is illustrated in Fig. 5. Consider that the RFS-U message from node 4 is not successfully received by node 2 in slot  $s_7$ . Node 4 is aware that node 2 has two child nodes. As per Rule SR-1, it retransmits the RFS-U message in slot  $s_{13}$ . Fig. 5 also shows the scenario where RFS-U message from node 6 is not successfully received by node 2 in slot  $s_{10}$ . Without DLS retransmission from node 2 in slot  $s_{12}$ , node 6 would have retransmitted the RFS-U message in slot  $s_{16}$ . However, the DLS retransmission from node 2 (as per Rule SR-3), informs node 6 that node 4 has been successful. Hence, it retransmits the RFS-U message in slot  $s_{13}$ , as per Rule SR-1.

**Policy for Schedule Termination** – The scheduling phase is terminated by the controller once all of its child nodes have been successfully scheduled in the uplink.

### E. Single-hop Operation

Although GALLOP has been designed for multi-hop operation, it also has the capability of operating in single-hop environments. The proposed distributed scheduling framework is transparent to the network topology. Hence, it can be directly

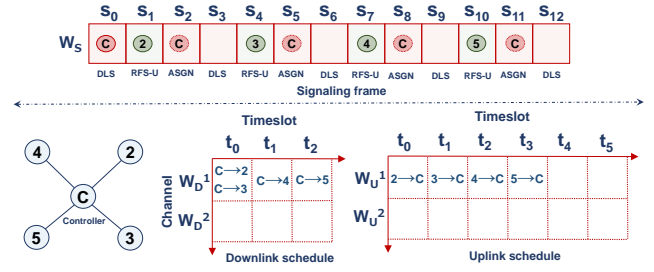


Fig. 6. Distributed scheduling of GALLOP for single-hop operation.

applied in single-hop scenarios without any modifications. Fig. 6 illustrates the distributed scheduling procedure and the constructed schedule for single-hop operation. The scheduling process, which is initiated by the controller, follows the aforementioned policies for downlink and uplink signaling and parent-child handshake. We assume that the controller has distinct messages for nodes 2 and 3, node 4 and node 5. Hence, it takes three timeslots on the downlink channel. In the uplink, each leaf node is allocated a distinct timeslot for communication with the controller.

### F. Frequency/Channel Hopping

GALLOP implements two different frequency/channel hopping techniques. In *phase-slotted* hopping, frequency hopping is performed on a phase-by-phase basis. The actual frequency/channel for the phase pertaining to data transmissions or retransmissions is given by  $\{(AP\_No + C\_Off) \bmod N_C\}$ , where  $AP\_No$  is the absolute phase number,  $C\_Off$  is the channel offset,  $N_C$  is the total number of channels and  $\bmod(\cdot)$  denotes the modulo operation. In *time-slotted* hopping frequency/channel hopping is performed at timeslot level in a similar manner.

## IV. GALLOP – RETRANSMISSION TECHNIQUES

In GALLOP, cyclic information exchange between the controller and slaves/devices occurs over the built downlink and uplink schedules. A transmission in either downlink or uplink may fail due to interference or fading. Retransmissions, which are handled in the final phase of GALLOP, are crucial in achieving high reliability. Note that recovery of MAC layer transmission failures in multi-hop control networks lead to the overhead-determinism-reliability (ODR) trade-off. GALLOP implements three different MAC layer retransmission techniques that distinctively account for the ODR trade-off.

### A. Schedule Duplication

The first technique is a manifestation of packet duplication functionality, which is achieved through duplicating the transmission schedule in time domain. Further, this technique integrates channel diversity with packet duplication. The two transmissions of the same packet at two different time instances and on two different frequencies provides high reliability. The main motivation for schedule duplication is to guarantee deterministic performance. Besides, it does not incur any overhead. Schedule duplication can be achieved in two different ways which are illustrated in Fig. 7. The *first option*

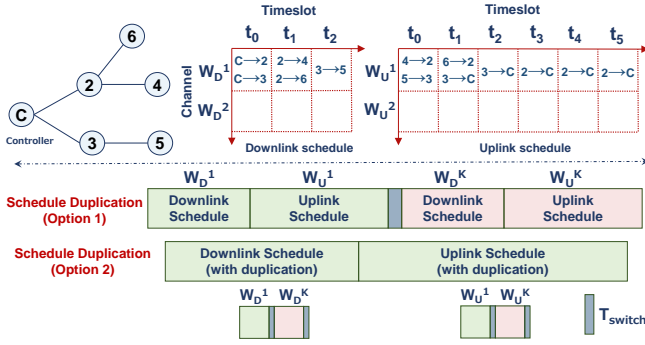


Fig. 7. Schedule duplication technique and the two options for duplication.

is to duplicate the transmission schedule. The first round of transmissions takes place as per the constructed schedule. In the second round, the downlink and uplink transmission phases are repeated, as per the existing schedule, with each phase going on a different channel. Note that there is a fixed channel switching delay between individual rounds. While this approach improves reliability in a deterministic manner, it also doubles the latency. The schedule can be repeated more than once as long as the latency bound is not violated. The *second option* is to build the schedule in a way that accounts for packet duplication. During the schedule construction phase, each node requests one extra timeslot per transmission, which is used for duplication. To incorporate channel diversity, the second transmission of the same packet goes on a different channel. This requires a fixed channel switching delay between adjacent timeslots. This approach also provides higher reliability in a deterministic manner. However, its latency could be lower than the previous option due to the fact that GALLOP exploits opportunities for parallel transmissions in the schedule.

## B. Retransmission Scheduling

The second technique builds a schedule for MAC layer transmission failures. It also exploits cooperative multi-user diversity and opportunistic network coding techniques. Note that in multi-hop wireless networks, any parent node needs to forward its own information along with that of its child nodes. In GALLOP, a parent node maintains a certain order of transmissions on the allocated (uplink) timeslots. It uses the first timeslot for its own information. Subsequent timeslots are used for forwarding the information of child nodes in the order of priority. For example, in Fig. 4 node 2 uses timeslot  $t_3$  for transmitting its own information, and  $t_4$  and  $t_5$  for forwarding the information of nodes 4 and 6, respectively. Each parent node also enumerates packets in sequence of transmission, e.g., node 2 will mark its transmissions in timeslots  $t_3$ ,  $t_4$ , and  $t_5$  as 1, 2, and 3, respectively. To exploit cooperative multi-user diversity, GALLOP relies on certain nodes to act as relays for others. The relay selection method is described later. The relay node for any arbitrary node is selected by its parent node from its child nodes. The relay nodes overhear during the transmission schedule phase and buffer the overheard packets from the nodes for which they act as relays. The need for building a retransmission schedule is ascertained by the controller. At the end of the transmission schedule, the controller

determines if a transmission from any of its child nodes is missing. The missing transmission could be of the controller's child or of any other node further away in the multi-hop topology. If one or more transmissions are found missing, the controller generates a GALLOP negative acknowledgement (G-NACK) message which contains the IDs of its child nodes with failed transmissions along with the number of the missing transmission. The subsequent parent nodes generate their own G-NACK messages if required. The G-NACK messages are disseminated in the network through the downlink schedule. The signaling for retransmission schedule follows the same handshake policy as explained earlier. Unlike the original schedule building phase, there are only two types of signaling slots on the signaling channel, i.e., RFS slots and ASGN slots which are numbered as  $\{s_0, s_2, s_4, \dots\}$  and  $\{s_1, s_3, s_5, \dots\}$ , respectively.

**Retransmission Scheduling Signaling Policy** – The retransmission scheduling signaling policy dictates signaling channel access for building the retransmission schedule. It consists of the following rules.

**Rule RS-1:** Any node  $m \in \mathcal{M}$  ( $m \neq$  controller) accesses the signaling channel in the earliest available slot, as per its local knowledge, if it has the missing transmission in its buffer.

**Rule RS-2:** Any parent node  $r \in \mathcal{R}$  ( $r \neq$  controller) with a failed transmission from any of its child nodes accesses the signaling channel in the earliest available slot, as per its local knowledge, after it has allocated timeslots for the missing transmissions.

**Rule RS-3:** The controller terminates the signaling after it has allocated timeslots for all the missing transmissions.

The retransmission scheduling technique is explained by distinguishing the following cases which are illustrated in Fig. 8. Note that the topology in Fig. 8 is different than that in Fig. 4 as the controller has an additional child node (node 4 which only has the controller and node 2 in its neighborhood). Hence, the constructed schedule is slightly different.

1) *Case A:* Assume that at the end of the transmission schedule, the second transmission from node 2 was missing at the controller. The controller sends a G-NACK message to its child nodes in the first timeslot of the downlink schedule. Based on the G-NACK message, node 3 determines that it does not need to engage in retransmission scheduling phase. However, node 2 needs to participate in the retransmission scheduling to recover its missing transmission. It knows that the second transmission (indicated in the G-NACK) was meant to be used for forwarding node 6's information. This transmission could be in its own buffer, provided the transmission from node 6 to node 2 in timeslot  $t_0$  of the uplink schedule was successful. We assume that this transmission was successful and it is available in node 2's buffer. Therefore, it sends an empty G-NACK message to its child nodes in the second timeslot of the downlink schedule. The empty G-NACK notifies its child nodes that their transmissions were successful. Similarly, node 3 sends an empty G-NACK to node 5 in the third timeslot of the downlink schedule. After the end of the downlink schedule phase, all nodes switch to the signaling channel. Based on Rule RS-1, node 2 will access slot  $s_0$  of the signaling channel  $W_S$  to request timeslots for the missing



transmission through an *RFS retransmission scheduling* (RFS-RS) message. To exploit cooperative multi-user diversity, each node with a failed transmission in its buffer will request two timeslots. Hence, node 2 requests timeslots  $t_0$  and  $t_1$  on the retransmission channel  $W_R$ . Since the controller finds no conflict, it confirms the requested allocation as per Rule H-2 by sending an ASGN message in slot  $s_1$ . After successful allocation, the controller terminates the scheduling phase, as per Rule RS-3, by sending a specific downlink message.

After termination of the retransmission signaling phase, nodes switch to the retransmission channel. Recall that node 2 requested two timeslots. The first timeslot is used by a parent node to communicate with the relay. We assume that node 4 is the default relay for node 2. As relay nodes overhear, it is likely that the missing transmission from node 2 is in node 4's buffer. The missing transmission can be recovered via various types of cooperative transmissions employing the relay node.

**Cooperative Transmission 1** – The source node and the relay node simultaneously transmit the missing information. For instance, as shown in Fig. 8, node 2 and node 4 simultaneously transmit in timeslot  $t_1$ . This provides reliability enhancement by providing a gain in received power, if the two transmissions are tightly time synchronized within half the symbol period. This phenomenon, which has been exploited by a number of recent synchronous/concurrent transmission-based flooding protocols [28], [29], is referred to as *constructive interference* (CI) in literature.

**Cooperative Transmission 2** – The relay node performs a simple network coding (SNC) operation by encoding the missing information with any *a priori* information at the controller. Let,  $Y_{22}$  denote the missing transmission (second transmission of node 2). The relay node encodes  $Y_{22}$  and its own uplink transmission,  $Y_{41}$  (that was successfully received by the controller), by performing an XOR operation (i.e.,  $Y_{22} \oplus Y_{41}$ ), and transmitting the encoded information in timeslot  $t_1$  to the controller. From a reliability perspective, the SNC operation provides two distinct benefits: (i) simple XOR-based coding has been shown to introduce a gain as compared to the case of simply forwarding overheard information [30], and (ii) relay's transmission provides path diversity.

It is also possible to integrate cooperative transmissions 1 and 2. Besides, cooperative multi-user diversity can be achieved through physical layer network coding (PLNC) [31]. Similar to cooperative transmission 1, node 2 and node 4 simultaneously transmit  $X_{22}$  in timeslot  $t_1$ ; however, the controller decodes the missing information based on *a priori* mapping for interpreting the combined received signal.

2) *Case B*: Similar to the previous case, the second transmission from node 2 was missing at the controller; however, it was not available in the buffer of node 2. Therefore, node 2 sends a G-NACK to its child nodes indicating that the first transmission from node 6 is missing. After the downlink schedule phase ends, nodes switch to the signaling channel. As node 6 is the leaf node, it is the source node for the missing transmission. In this case we assume that node 6 sent an uplink message (in timeslot  $t_1$ ); however, it was not successfully received by node 2. As per Rule RS-1, node 6 requests timeslots  $t_0$  and  $t_1$ , on the retransmission channel

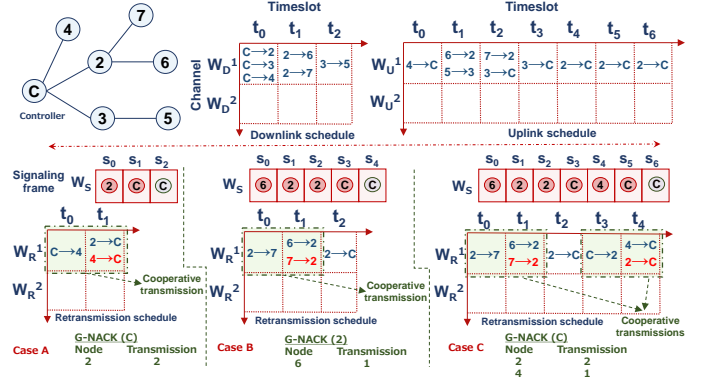


Fig. 8. Retransmission scheduling technique and the schedule construction process in different cases.

$W_R$ , by sending an RFS-RS message in slot  $s_0$ . Node 2 confirms the requested allocation in slot  $s_1$ , as per Rule H-2. As the transmission from node 6 needs to be forwarded to the controller, node 2 requests timeslot  $t_2$  by sending an RFS-RS message in slot  $s_2$ , as per Rule RS-2. After confirming the requested allocation, the controller terminates the scheduling phase. We assume that node 7 is the default relay for node 6. Therefore, timeslots  $t_0$  and  $t_1$  are used for cooperate transmission, exploiting CI, to recover the failed transmission of node 6. In the subsequent timeslot ( $t_2$ ), node 2 forwards this information to the controller. Node 2 can either simply transmit this information or it can perform a SNC operation.

3) *Case C*: Consider that at the end of the transmission schedule, the second transmission from node 2 and the only transmission from node 4 were missing at the controller. The controller indicates these in the G-NACK message to its child node. Similar to the previous case, the missing transmission from node 2 is not available in its buffer. However, the missing transmission from node 4 is available in its own buffer. Node 2 sends a G-NACK to its child nodes indicating that the first transmission from node 6 is missing. During the retransmission phase, nodes also overhear G-NACK messages to maintain local knowledge. Although node 4 has the missing transmission in its buffer, it would abstain from accessing the first slot of the signaling channel as it is not free as per its local knowledge. The G-NACK from the controller informs node 4 that node 2 (a higher priority node) has missing transmission(s). Further, the G-NACK overheard from node 2 informs node 4 that the missing transmission from node 2 is not in its own buffer. Hence, node 4 ascertains that the first two RFS slots can potentially be occupied as node 2 would request timeslots for itself in case the missing transmission is present in the buffer of its child node. Similar to the previous case, we assume that the missing transmission from node 6 is available in its own buffer. As per Rule RS-1, it requests timeslots  $t_0$  and  $t_1$  in an RFS-RS message in slot  $s_0$ . Node 2 confirms the requested allocation in slot  $s_1$ . As per Rule RS-2, node 2 requests timeslot  $t_2$  by sending an RFS-RS message in slot  $s_2$ . The controller confirms the requested allocation in slot  $s_3$ . In slot  $s_4$ , node 4 requests timeslots  $t_3$  and  $t_4$ , which are the earliest available timeslots as per its local knowledge. The controller confirms the requested allocation and terminates the scheduling phase subsequently. Once the signaling phase



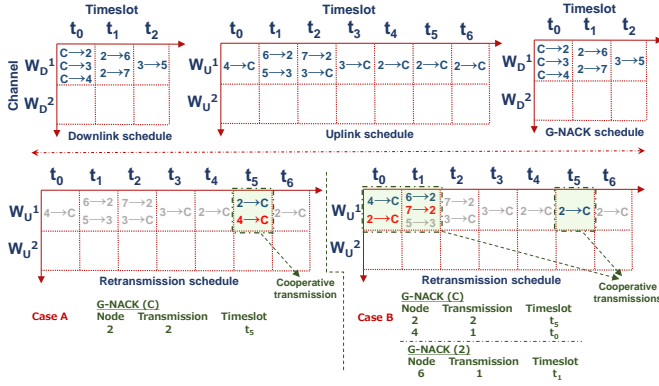


Fig. 9. Schedule extrapolation technique and the retransmission schedule in different cases for the topology in Fig. 8.

is over, nodes switch to the retransmission channel. Note that node 4 is the default relay for node 2 and vice versa, and node 7 is the default relay for node 6. First, the missing transmission of node 6 is recovered cooperatively. Timeslot  $t_0$  is used for parent-relay communication. In timeslot  $t_1$ , node 7 and node 6 simultaneously transmit the missing information which leads to CI. Timeslot  $t_2$  is used by node 2 to forward node 6's information to the controller. Finally, timeslots  $t_3$  and  $t_4$  are used to recover node 4's missing information in a similar way.

4) *Case D*: This case is similar to Case B except that node 6 does not have the missing transmission in its buffer. This could happen if the downlink transmission from node 2 to node 6 failed. Consequently, node 6 did not transmit in the uplink. After receiving the G-NACK from node 2, node 6 determines the need for downlink transmission. In this case, it would request three timeslots. The first timeslot ( $t_0$ ) is used for parent-relay communication where node 2 will inform node 7 of the need for cooperative downlink transmission. In the second timeslot ( $t_1$ ), both node 2 and node 7 simultaneously transmit the downlink information. The third timeslot ( $t_3$ ) is used by node 6 to transmit its uplink information to node 2.

The retransmission scheduling technique provides very high reliability. It also provides flexibility as the retransmission schedule is customized for recovering the missing transmissions only. However, it encompasses a non-deterministic signaling component and the overhead of building a schedule.

### C. Schedule Extrapolation

The third technique integrates the key benefits of the first two techniques. It extrapolates the transmission schedule for recovering missing transmissions through cooperative transmissions *without building a retransmission schedule*. This is achieved by embedding some extra information in the G-NACKs which are disseminated through the downlink schedule. The need for retransmissions is ascertained by the controller. However, retransmissions are handled based on the transmission schedule. The schedule extrapolation technique is explained through the following cases which are illustrated in Fig. 9.

1) *Case A*: Consider the scenario wherein node 2's second transmission was missing at the controller at the end of the transmission schedule; however, it was available in node 2's

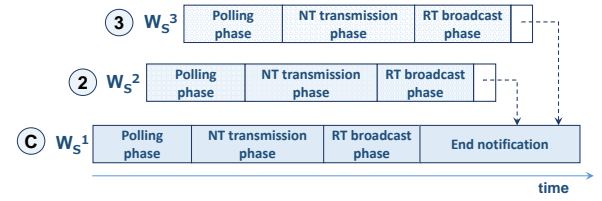


Fig. 10. Relay selection technique in GALLOP (same topology as Fig. 4).

buffer. The controller generates a G-NACK message indicating the missing transmission. Unlike retransmission scheduling technique, the controller also embeds the timeslot information of the missing transmission in the G-NACK message, which in this case is  $t_5$ . The G-NACK from the controller also informs the relay node (node 4) to engage in a cooperative transmission at timeslot  $t_5$ . Therefore, in timeslot  $t_5$ , both node 4 and node 2 simultaneously transmit the missing information to the controller which leads to CI. Note that a schedule for retransmission is not explicitly constructed. The original uplink schedule is duplicated for recovering failed transmissions while exploiting cooperative transmissions for enhanced reliability. It is important to mention that the successful transmissions in the previous round may not be retransmitted (duplicated).

2) *Case B*: Consider that node 2's second transmission and the only transmission of node 4 were missing at the controller at the end of the transmission schedule. The controller generates a G-NACK message indicating these transmissions and the respective timeslots. We assume that the missing transmission from node 4 was available while that of node 2 was not available in their respective buffers. Hence, node 2 generates a G-NACK message indicating the missing transmission of node 6 and the associated timeslot. The G-NACK from the controller informs nodes 2 and 4 to engage in cooperative transmissions for each other in timeslots  $t_0$  and  $t_5$ , respectively. The G-NACK from node 2 informs node 7 to engage in a cooperative transmission for node 6 in timeslot  $t_1$ . Note that any relay node would not engage in a cooperative transmission if it does not have the missing information in its buffer. In timeslot  $t_0$  of the retransmission schedule, node 4 and node 2 simultaneously transmit the missing information which leads to CI. Similarly, node 6 and node 7 engage in a cooperative transmission in timeslot  $t_1$ . Finally, node 2 forwards node 6's information to the controller in timeslot  $t_5$ . Note that, node 2 can also forward the missing information based on the aforementioned SNC operation.

The schedule extrapolation technique achieves very high reliability while providing deterministic performance. However, it may not provide the same level of flexibility as the retransmission scheduling technique.

### D. Relay Selection

GALLOP implements a simple relay selection technique (illustrated in Fig. 10) which is based on link-level measurements. It begins by the controller polling each of its child nodes by transmitting an empty RFS message on the default signaling channel. Each child node responds with an empty ASGN message. The neighboring child nodes of the controller

which successfully receive the ASGN message add the ID of the polled child along with the received signal-to-noise ratio (SNR) in a neighbor state table (NT). Each child node only records  $N_b$  strongest neighbors. After successfully polling all child nodes, the controller transmits a DLS message which contains a schedule for its child nodes on the default signaling channel. Based on the schedule information, each child node reports its NT to the controller. Upon receiving the NTs, the controller computes a relay state table (RT) that includes a relay node for each child node. The controller picks the relay node based on the highest SNR from every child's NT. It broadcasts the RT on the default signaling channel. Each non-leaf child node repeats the aforementioned operation for its child nodes on a different channel after receiving the RT from the controller. For parallel operation of multiple branches, the controller allocates a subset of orthogonal channels to all of its child nodes. The channel information can potentially be embedded in the schedule information for receiving the NTs. The procedure continues in the downward direction such that each parent node allocates a subset of orthogonal channels to its child nodes. A leaf node notifies its parent by transmitting an uplink signaling message that indicates end of relay selection operation, on the respective channel. The relay selection process completes once the controller has received an uplink signaling message from all of its child nodes. Relay selection procedure can also be realized in an online manner based on overhearing during data transmission phases. If a node successfully overhears from a neighbor (with the same default parent), with an average SNR (over a fixed number of phase) above a certain threshold, it notifies its parent to act as a relay for the neighbor. The information exchange pertaining to relay selection can be piggybacked on uplink/downlink transmissions.

## V. GALLOP – CONVERGENCE TIME ANALYSIS

We adopt an SNR-based model for link outage, where a transmission is successful if the instantaneous SNR exceeds a threshold. We consider the case of an arbitrary parent node  $p$  with  $K$  directly connected child nodes uniformly distributed in its coverage radius, denoted by  $R_p$ . Let  $\gamma_{\text{sig}} = \mathcal{P}^t |h|^2 d^{-\alpha} / \sigma^2$  denote the instantaneous SNR of a signaling transmission in either downlink or uplink such that  $\mathcal{P}^t$  denotes the transmit power,  $h$  denotes the channel fading coefficient,  $d$  denotes the distance,  $\alpha$  is the path loss exponent, and  $\sigma^2$  is the noise power. Let,  $P_o^{\text{sig}}$  denote the average outage probability for the signaling transmission which can be evaluated as

$$P_o^{\text{sig}} = \mathbb{E}_d [\mathbb{P} \{ \gamma \leq \beta \}] = \mathbb{E}_d [\mathbb{P} \{ |h|^2 \leq \beta \sigma^2 d^\alpha / \mathcal{P}^t \}], \quad (2)$$

where  $\beta$  is the threshold SNR for successful transmission and  $\mathbb{E}_d$  denotes the expectation over the distance. The probability density function (PDF) of the distance between the parent node and the  $k$ th child node is given by [32]

$$f(d, k) = \frac{(1 - d^2/R_p^2)^{K-k} (d^2/R_p^2)^{k-1} 2d}{B(K-k+1, k) R_p^2}, \quad (3)$$

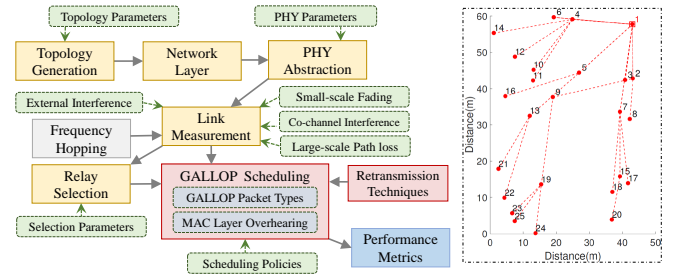


Fig. 11. Schematic block diagram of the GALLOP simulator.

where  $B(\cdot)$  is the Beta function. Using (3) and under the assumption of widely used Rayleigh fading,  $P_o^{\text{sig}}$  is given by

$$P_o^{\text{sig}} = \frac{2}{R_p^2} \int_0^{R_p} d [1 - \exp(-\zeta d^\alpha)] dd, \quad (4)$$

where  $\zeta = \beta \sigma^2 / \mathcal{P}^t$ . We define  $P_a^f$  as the probability of allocation failure for a node which is given by

$$P_a^f = [P_o^{\text{RFS}} + (1 - P_o^{\text{RFS}}) P_o^{\text{ASGN}}] \cdot (1 - P_o^{\text{DLS}}), \quad (5)$$

where  $P_o^{\text{RFS}}$ ,  $P_o^{\text{ASGN}}$  and  $P_o^{\text{DLS}}$  denote the average outage probability for RFS, ASGN and DLS messages, respectively, which can be calculated using (4).

Next, we find the average convergence time. In the ideal scenario of no link-level transmission failures, the convergence time (in terms of signaling slots) for constructing a schedule is given by  $\mathcal{T}_{\text{conv}}^I = 3K + 1$ . Let,  $w_o^k$  denote the access delay for the first RFS retransmission of the  $k$ th device. Then, the average access delay (based on signaling message retransmission policy) for successful allocation at first RFS retransmission can be calculated as

$$\begin{aligned} \mathbb{E}(w_o^k) &= \frac{3}{K} P_a^f (1 - P_a^f) \sum_{i=1}^K [(i-1) - i(1 - P_a^f)] \\ &= \frac{3}{2} P_a^f (1 - P_a^f) [(K-1) - (K+1)(1 - P_a^f)]. \end{aligned} \quad (6)$$

The average access delay for successful allocation at second or higher RFS retransmission can be calculated as

$$\begin{aligned} \mathbb{E}(w_r^k) &= 3 \sum_{j=2}^{\infty} j (P_a^f)^j (1 - P_a^f) \left[ \frac{1 + \Psi}{2} + \frac{1}{K} \sum_{i=1}^K (i-1) \right] \\ &= \frac{3(K + \Psi)}{2} \left[ \frac{2(P_a^f)^2 - (P_a^f)^3}{1 - P_a^f} \right]. \end{aligned} \quad (7)$$

Hence, the mean convergence time for an arbitrary parent node  $p$  with  $K$  directly connected child nodes is given by

$$\mathcal{T}_{\text{conv}} = \mathcal{T}_{\text{conv}}^I + \mathbb{E}(w_o^k) + \mathbb{E}(w_r^k), \quad (8)$$

where  $\mathbb{E}(w_o^k)$  and  $\mathbb{E}(w_r^k)$  are given by (6) and (7), respectively. Note that  $\mathcal{T}_{\text{conv}}$  reduces to  $\mathcal{T}_{\text{conv}}^I$  when  $P_a^f = 0$ , which is intuitive. The proposed framework can be integrated with spatial modeling techniques to achieve bounds on the overall convergence time of a multi-hop topology. As this is a complete topic in itself, it has been left as part of future work.

TABLE I  
PARAMETERS FOR PERFORMANCE EVALUATION

Parameter	Value	Parameter	Value
Noise Power	-174 dBm/Hz	Channel bandwidth	2 MHz
Transmit power	9 dBm	Path loss exponent ( $\alpha$ )	3.3
Slot duration	200 $\mu$ s	PHY layer	LE 2M

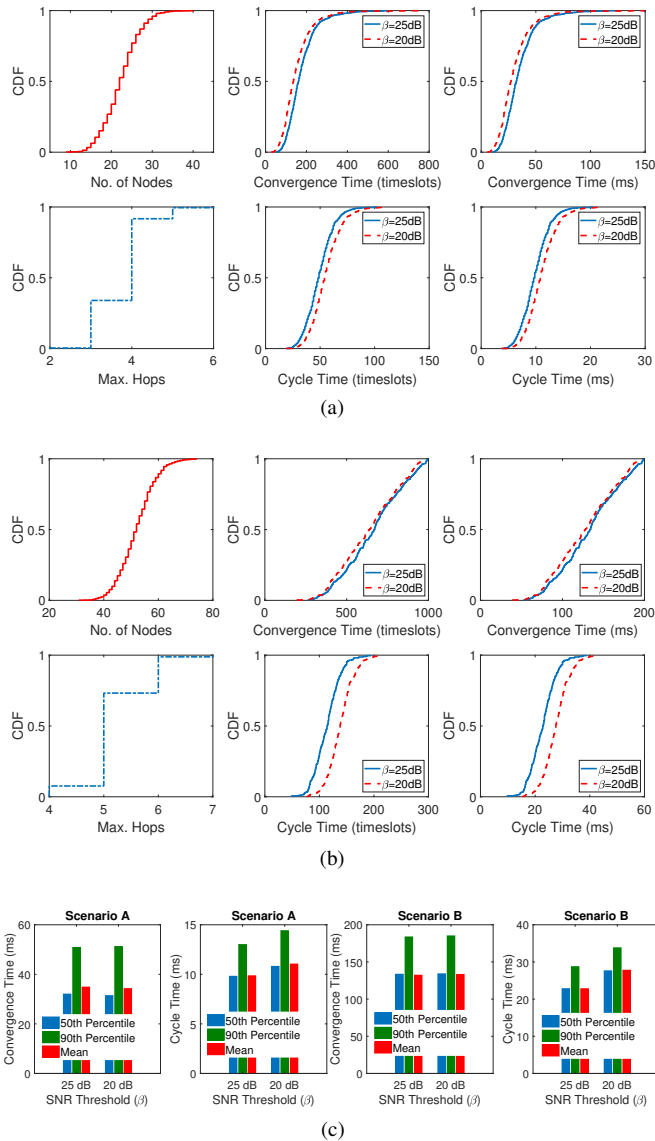


Fig. 12. Convergence time and cycle time performance for (a) *Scenario A* and (b) *Scenario B*. The statistics are shown in (c).

## VI. GALLOP – SYSTEM-LEVEL SIMULATIONS

We have developed a MATLAB-based simulator for system-level evaluation of GALLOP. The schematic of the simulator is shown in Fig. 11. We deploy a Poisson<sup>2</sup> distributed mesh topology of nodes in a region, which is transformed into a tree topology based on a routing protocol. We have implemented a simplified version of RPL [26] at the network layer such that each node is assigned a rank based on the Euclidean distance from the controller. A realization of the multi-hop

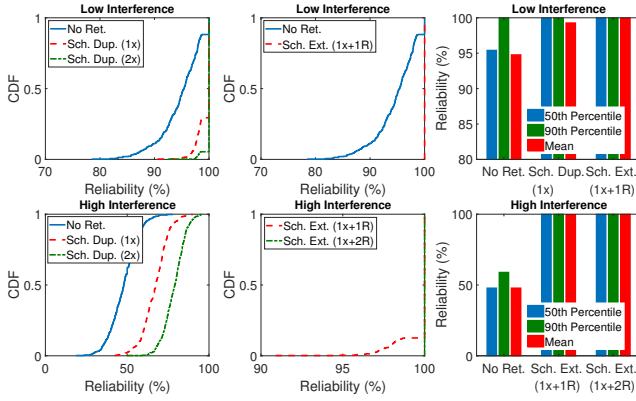
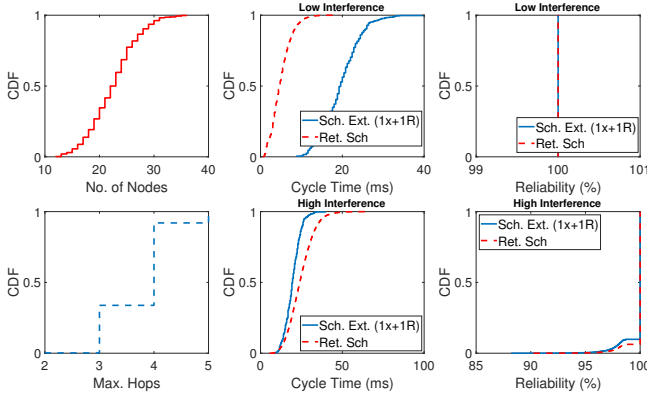
<sup>2</sup>We have used Poisson distributed topology as the Poisson point process is the most widely used spatial point process for modeling connectivity in wireless (cellular, ad-hoc, mesh, etc.) networks.

topology is shown in Fig. 11. The PHY abstraction block creates a PHY layer model based on various parameters. The link measurement block captures the channel model and accounts for small-scale Rayleigh fading, large-scale path loss, co-channel interference (collisions), and external interference. We adopt a well-known path loss model, commonly employed for Bluetooth, wherein the path loss (in dB) at a distance  $d$  is given by  $PL(d) = PL(d_0) + 10\alpha \log(d/d_0)$ , such that  $PL(d_0) = 58.1$  dB,  $d_0 = 8$  meters (m) and  $\alpha$  is the path loss exponent. The relay selection block implements the proposed relay selection technique. We have implemented GALLOP at the message level. The slot duration is set to 200  $\mu$ s as in our hardware implementation. Other parameters are given in TABLE I. We consider two scenarios for network topology and conduct Monte Carlo simulations on different multi-hop topologies. In *Scenario A*, nodes are Poisson distributed with a mean value of 20 in a square region of side 60 m. In *Scenario B*, nodes are Poisson distributed with a mean value of 50 in a square region of side 80 m.

Fig. 12 shows the convergence time (which is defined as the time taken to build the schedule) and the cycle time for both scenarios based on 1000 iterations, with a different topology in each iteration. In *Scenario A*, where 10 to 40 nodes are distributed with a maximum of 2 to 6 hops from the controller, GALLOP achieves a mean convergence time of 36 ms (180 slots) with a 90th percentile of 50 ms (250 slots), for an SNR threshold ( $\beta$ ) of 25 dB. In *Scenario B*, where 30 to 75 nodes are distributed with a maximum of 4 to 7 hops from the controller, the mean convergence time and the 90th percentile is 130 ms and 182 ms, respectively, for  $\beta = 25$  dB. The convergence time decreases in both scenarios for  $\beta = 20$  dB due to less stringent link-level requirements for the success of signaling messages.

In *Scenario A*, GALLOP achieves a mean cycle time of 9.5 ms (90th percentile of 13 ms), for  $\beta = 25$  dB. With a similar  $\beta$ , the mean cycle time is 22 ms (90th percentile of 29 ms) in *Scenario B*. The cycle time increases in both scenarios when  $\beta = 20$  dB. This is because a lower value of  $\beta$  reflects a relatively denser environment. Hence, there are less parallel transmission opportunities which leads to increase in length of the overall schedule. Results demonstrate that GALLOP adapts the schedule as per network conditions due to local overhearing. In dense networks, it builds a sequential schedule for avoiding conflicts. In sparse networks, it exploits opportunities for parallel transmissions.

Next, we evaluate the reliability (in terms of packet delivery) performance and investigate the robustness of different retransmission techniques. We implement a spatio-temporal model for external Wi-Fi interference. From a spatial perspective, the distance of a receiver from an interfering Wi-Fi access point (AP) is uniformly distributed between 1 m and 25 m. From a temporal perspective, the traffic of an AP is modeled as a two-state independent and identically distributed random process wherein the duration of busy (ON) and idle (OFF) periods is exponentially distributed with a mean of  $\mu_{ON}$  and  $\mu_{OFF}$ , respectively. We consider two interference scenarios. In *low interference*, each link is interfered by a single AP, transmitting at 14 dBm with  $\mu_{ON} = 0.25$  ms and  $\mu_{OFF} = 0.5$  ms. In


 Fig. 13. Reliability performance of different techniques for *Scenario A*.

 Fig. 14. Performance comparison of retransmission scheduling and schedule extrapolation techniques for *Scenario A*.

*high interference*, each link is interfered by up to three APs, transmitting at 20 dBm with  $\mu_{ON} = 1.5$  ms and  $\mu_{OFF} = 0.5$  ms. Fig. 13 shows the reliability performance of different retransmission techniques for *Scenario A*. Under low interference, GALLOP achieves a mean reliability of 94.79% when no retransmissions are enabled. However, schedule duplication as well as schedule extrapolation improve reliability. With one and two schedule duplications, the mean reliability increases to 99.19% and 99.8%, respectively, and with schedule extrapolation to 100%. In high interference, the mean reliability is 48% (90th percentile of 59%) when no retransmissions are enabled. With one and two schedule duplications, the mean reliability increases to 67% (90th percentile of 76.09%) and 78.7% (90th percentile of 86.55%), respectively. We limit our evaluation to cooperative transmission 1. With schedule extrapolation (employing cooperative transmission 1), the mean reliability is 99.68% (90th percentile of 100%). The mean reliability with schedule extrapolation increases to 100% if up to two relay nodes are used. The results demonstrate the effectiveness of cooperative transmissions for very high reliability. Similar reliability gain has been achieved in *Scenario B*. Fig. 14 compares the performance of retransmission scheduling and schedule extrapolation. Both techniques achieves very high reliability under low as well as high interference. The main difference comes in cycle time performance. Schedule extrapolation achieves a mean cycle time of 19.8 ms (99 timeslots) with a 90th percentile of 26.8 ms (134 timeslots). In low interference, retransmission scheduling achieves a mean cycle

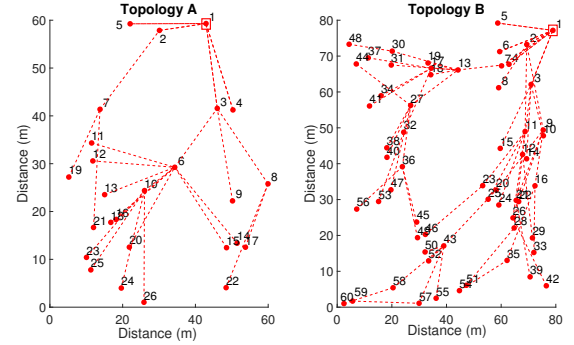


Fig. 15. Topology A and Topology B. Node 1 is the controller.

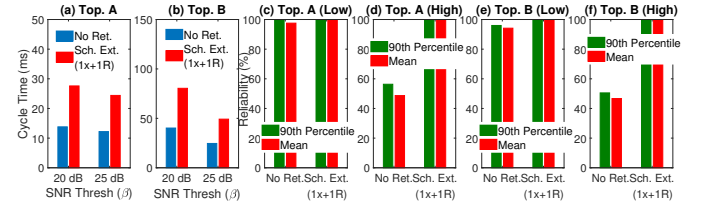


Fig. 16. Cycle time (in (a) – (b)) and reliability (in (c) – (f)) performance for Topologies A and B.

time of 5 ms (25 timeslots) with a 90th percentile of 8.4 ms (42 timeslots). However, under high interference, the mean cycle time increases to 24.8 ms (124 timeslots) with a 90th percentile of 35 ms (175 timeslots). This increase is due to higher convergence time for constructing the retransmission schedule. Retransmission scheduling is 75% better on average in terms of cycle time under low interference. However, under high interference, it performs 20% worse on average in terms of cycle time.

We also evaluate the performance of GALLOP on two distinct topologies shown in Fig. 15. Topology A comprises 26 nodes with maximum of 4 hops whereas Topology B consists of 60 nodes with maximum of 6 hops. The cycle time and reliability performance for both topologies is shown in Fig. 16. Key results are summarized as follows. For  $\beta = 25$  dB, the cycle time for Topology A is 12.2 ms with no retransmissions. The cycle time doubles to 24.4 ms with schedule extrapolation. In a similar setting, the cycle time for Topology B is 24.6 ms with no retransmissions and 49.2 ms with schedule extrapolation. In low interference, the mean reliability with no retransmissions is 97.2% (90th percentile of 100%) and 94.15% (90th percentile of 95.97%) for Topology A and Topology B, respectively. With schedule extrapolation, the mean reliability is 100%. In high interference, the mean reliability with no retransmissions is 48.6% (90th percentile of 56.3%) and 46.69% (90th percentile of 50.5%) for Topology A and Topology B, respectively. Using schedule extrapolation, the mean reliability is 99.97% for Topology A and 99.83% for Topology B, respectively.

GALLOP is equally capable of single-hop operation. Its distributed scheduling algorithm is agnostic to the nature of topology. Fig. 17 shows the single-hop performance and its benchmarking against WISA. In a single-hop network comprising 30 – 65 nodes within controller's coverage, the mean cycle time of GALLOP with schedule extrapolation is



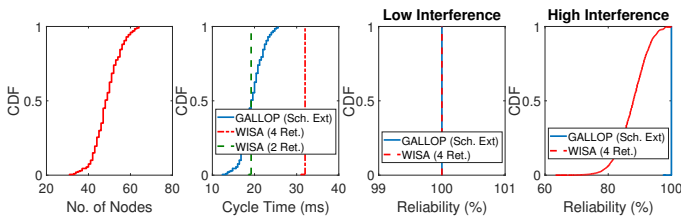


Fig. 17. Single-hop performance of GALLOP ( $\beta = 25$  dB).

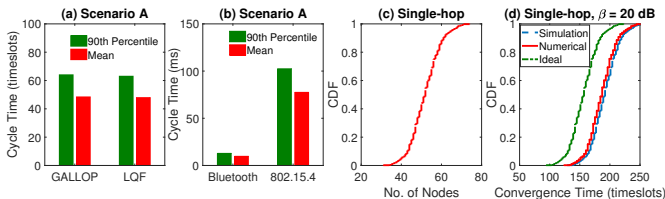


Fig. 18. GALLOP evaluation from (a) algorithmic and (b) hardware aspects. Scenario and results for convergence time are shown in (c) and (d).

98 timeslots or 19.6 ms (90th percentile of 114 timeslots or 22.8 ms). On the other hand, WISA provides a cycle time of 160 timeslots (32 ms) and 96 timeslots (19.2 ms) with 4 and 2 mandatory retransmissions, respectively. Both technologies achieve similar reliability of 100% under low interference. Under high interference, WISA with 4 retransmissions achieves a mean reliability of 87.6% (90th percentile of 93.75%), whereas GALLOP achieves a mean reliability of 99.94% (90th percentile of 100%). Results demonstrate that GALLOP outperforms WISA, especially in terms of reliability performance while providing similar or better latency performance.

Fig. 18 captures the performance of GALLOP from different aspects. First, it evaluates the efficiency of distributed scheduling which is benchmarked against the *longest queue first* (LQF) algorithm [33], also known as *greedy maximal scheduling*. LQF is a centralized algorithm and often used as a heuristic for optimal performance. As per LQF, nodes are sorted in a descending order with respect to their queue lengths. The node with the longest queue is allocated the current timeslot. Other nodes which can transmit without causing conflict are also allocated the same timeslot. For *Scenario A*, LQF provides a *schedule duration* of 47.9 timeslots with a 90th percentile of 62.8 timeslots whereas GALLOP provides a mean cycle time of 48.4 timeslots with a 90th percentile of 64.5 timeslots. The results demonstrate that distributed scheduling of GALLOP provides a near-optimal performance despite its practicality and simplicity. Note that LQF is centralized in nature and requires queue length information for all the nodes in the network. LQF is also not control-aware like GALLOP. While LQF calculates an optimal schedule for a given topology, it cannot ensure minimal cycle time. Fig. 18 also shows that GALLOP would provide at least 8 times better performance, in terms of minimum cycle time, on a LE 2M PHY as compared to IEEE 802.15.4 PHY which is used by WirelessHART. Fig. 18 also shows the convergence time performance based on numerical and simulation results. The simulation results closely follow the numerical results and validate the accuracy of modeling convergence time.

## VII. GALLOP – HARDWARE IMPLEMENTATION

We have implemented GALLOP on the Nordic Semiconductor nRF52840-PDK platform (<https://www.nordicsemi.com/eng/Products/nRF52840>) which is built around a 32-bit ARM Cortex-M4F CPU with 1 MB flash and 256 kB RAM on chip. The embedded 2.4 GHz transceiver supports multiple protocols. GALLOP has been implemented on the LE 2M PHY of Bluetooth 5. However, it has been tested on the LE Coded PHY (125 kbps) as well. Our GALLOP implementation adopts an enhanced version of Glossy [34] and the Atomic stack [35] ported to the nRF52840 radio for multi-hop time synchronization. Following time synchronization, GALLOP initiates a time-slotted operation that is strictly enforced. The state machine is driven by radio and timer interrupts. It can change on three distinct events: packet successfully received, timeslot start and packet transmitted. The transmission decisions are handled on-the-fly at the end of every slot based on current state and packets queued for next available slot of the correct type. Each transmit slot is partitioned into pre-processing and transmission preparation, radio ramp-up and transmission and post-processing and protocol state operation. For each device, GALLOP uses an 8-bit ID which is generated by a hash function of its address.

We have conducted performance evaluation GALLOP over a testbed of Nordic nRF52840 devices deployed over two floors of our office (covering approximately 600 square meters). The testbed devices experience interference from Wi-Fi APs and other Bluetooth devices operating in office premises. We consider different multi-hop topologies which are shown in Fig. 19. Each topology consists of a single controller and multiple slave nodes. Topology 1 consists of 9 slaves with one 2-hop connection. Topology 2 comprises 11 slaves with two 2-hop connections. Topology 3 consists of 9 slaves with one 3-hop connection and one 2-hop connection. Topology 4 comprises 7 slaves in single-hop connectivity. In addition to these topologies, there is a Topology 5 which consists of 5 slave nodes with one 2-hop connection. Topology 5 is only used for testing the performance of LE Coded PHY.

### A. Evaluation on LE 2M PHY

We consider a bi-directional traffic model with cyclic information exchange where the controller sends command messages in the downlink and slave nodes respond back in the uplink. The GALLOP MAC protocol data unit (PDU) is 16 bytes in length. The overall packet size is 24 bytes as the LE 2M PHY has an 8 byte overhead. The minimum required slot duration is 136  $\mu$ s which accounts for a 40  $\mu$ s transmit/receive turnaround time for the nRF52840 radio. We have fixed the timeslot duration to 200  $\mu$ s to account for additional software delays. The transmit power is 9 dBm.

We have evaluated the convergence time performance of GALLOP based on 3000 iterations over our testbed. Key results are summarized in TABLE II. The results demonstrate the viability of distributed scheduling for both multi-hop and single-hop topologies. The results also demonstrate the capability of fast convergence (on the order of few ms) for building a schedule. It is emphasized that the schedule for

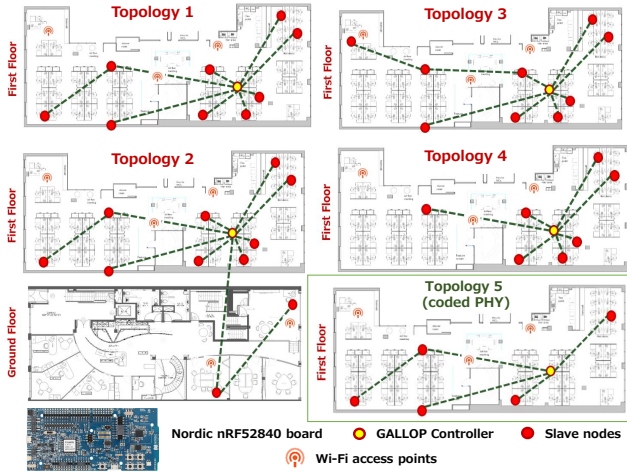


Fig. 19. Testbed topologies for multi-hop and single-hop performance evaluation of GALLOP.

TABLE II  
SUMMARY OF TESTBED EVALUATION (CONVERGENCE TIME)

Topology	Convergence Time (Mean)	Convergence Time (90th Percentile)
Topology 1	60.87 timeslots (12.17 ms)	63 timeslots (12.6 ms)
Topology 2	67.19 timeslots (13.43 ms)	69 timeslots (13.8 ms)
Topology 3	56.4 timeslots (11.28 ms)	60 timeslots (12 ms)
Topology 4	21.05 timeslots (4.21 ms)	21 timeslots (4.2 ms)

cyclic exchange needs to be built once for a specific topology. This is usually the case for most industrial applications, even for highway platooning. However, GALLOP is capable of rapid reconfiguration in dynamic environments with frequent topological changes.

The cycle time and reliability performance of GALLOP, which is summarized in TABLE III, has been evaluated over multiple phases of cyclic exchange. GALLOP provides a cycle time of 2.4 ms for Topology 1, 2.6 ms for Topology 2, 3 ms for Topology 3, and 1.6 ms for Topology 4. The reliability is measured in terms of mean packet delivery ratio (PDR) at the controller. In the absence of retransmissions and frequency hopping, the achieved reliability performance is not sufficient. For example, the achieved reliability for Topology 1 is 95.27%. However, the reliability improves significantly with schedule extrapolation and frequency hopping. For instance, the reliability for Topology 1 increases to 99.95%. Similar improvement in reliability has been achieved for other topologies as well. The evaluation reveals that cooperative transmissions are crucial for very high reliability. For example, in case of Topology 1, schedule extrapolation with no frequency hopping still achieves a reliability of 99.73%.

We have conducted a performance comparison of GALLOP against the standard Bluetooth mesh protocol [36]. On the same testbed, we consider a mesh topology of 15 nodes with a maximum of 3 hops. Bluetooth mesh protocol is based on a *managed flooding* technique wherein a message injected in the network is potentially forwarded by multiple relay nodes. A source node broadcasts data on three distinct channels (known as advertising channels) which are randomly scanned by the relay nodes. We consider a closed-loop control scenario as

TABLE III  
SUMMARY OF TESTBED EVALUATION (LE 2M PHY)

Topology	Phases	Cycle Time	Successful Packets	PDR
<b>No Retransmissions; No Frequency/Channel Hopping</b>				
Topology 1	2013	12 timeslots (2.4 ms)	17260	95.27%
Topology 2	1015	13 timeslots (2.6 ms)	10551	94.5%
Topology 3	1100	15 timeslots (3 ms)	9330	94.24%
Topology 4	1100	8 timeslots (1.6 ms)	7538	97.9%
<b>Schedule Extrapolation with Frequency/Channel Hopping</b>				
Topology 1	2003	24 timeslots (4.8 ms)	18018	99.95%
Topology 2	1000	26 timeslots (5.2 ms)	10918	99.25%
Topology 3	1026	30 timeslots (6 ms)	9190	99.52%
Topology 4	2006	16 timeslots (3.2 ms)	13976	99.53%
<b>Schedule Extrapolation without Frequency/Channel Hopping</b>				
Topology 1	1000	24 timeslots (4.8 ms)	8976	99.73%
Topology 4	1003	16 timeslots (3.2 ms)	6971	99.29%

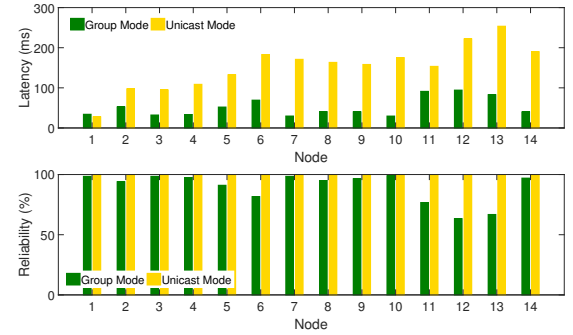


Fig. 20. Performance evaluation of standard Bluetooth mesh solution.

employed for GALLOP. One of the nodes is the controller which transmits a control message of 10 bytes payload to all the slave nodes in the network. The slave nodes respond by transmitting a response message. In the *group* mode, the controller floods a group message to all the slave nodes, whereas in the *unicast* mode, the controller sends a control message to each slave node individually. The evaluation results are shown in Fig. 20. Note that the cyclic exchange is not complete until the controller has received messages from all slaves. Therefore, the worst-case latency is important, which is 253 ms and 94 ms, in case of unicast mode and group mode, respectively. The unicast mode achieves 100% reliability as the controller keeps transmitting until it has received acknowledgement from a slave node. For group mode, the controller transmits the message over three *advertising events*. It achieves a mean reliability of 89.6%. Results show that GALLOP outperforms Bluetooth mesh by several orders of magnitude in terms of latency (cycle time) while providing similar or better reliability.

### B. Evaluation on LE Coded PHY

We have tested the cycle time and reliability performance of GALLOP on the LE Coded 125 kbps PHY as well. The minimum required slot duration for a 16 byte PDU is 1.6 ms. To account for processing overheads, we have fixed the timeslot length to 2 ms. The transmit power is 9 dBm.

TABLE IV  
SUMMARY OF TESTBED EVALUATION (LE CODED PHY)

Topology	Phases	Cycle Time	Successful Packets	PDR
<b>No Retransmissions; No Frequency/Channel Hopping</b>				
Topology 5	293403	7 timeslots (14 ms)	1410920	96.18%
<b>Schedule Duplication without Frequency/Channel Hopping</b>				
Topology 5	99602	14 timeslots (28 ms)	497851	99.97%



Fig. 21. Testbed for GALLOP evaluation in dense environments.

TABLE IV summarizes the key results obtained from evaluation on Topology 5. We have evaluated the reliability of LE Coded PHY in the absence of channel hopping and schedule extrapolation. As shown by the results in TABLE IV, the LE Coded PHY incurs significantly higher latency as compared to the LE 2M PHY. In the absence of channel hopping and retransmissions, the achievable reliability is 96.18%. The reliability improves to 99.97% with schedule duplication. Note that the LE Coded PHY is more vulnerable to interference than the LE 2M PHY due to more time on the air.

### C. Evaluation in Dense Deployments

We have also evaluated the performance of GALLOP in dense deployments. Such deployments represent various control-centric industrial applications including motion control in factory automation (that requires connectivity on a single industrial machine) and wireless battery management systems (monitoring and control of individual battery cells). As shown in Fig. 21, we have deployed 30 Nordic nRF52840 boards inside a cabinet. This creates a single-hop topology with one controller and 29 slaves. We have fixed the timeslot duration for data transmission to 0.5 ms to transmit larger payloads while accounting for processing overheads. Our evaluation results, which are based on the LE 2M PHY, are summarized in TABLE V. As shown by the results, GALLOP achieved a reliability of 100% with one schedule duplication. The results also show the viability of the convergence of distributed scheduling in dense deployments.

TABLE V  
SUMMARY OF TESTBED EVALUATION (DENSE DEPLOYMENT)

Topology	Phases	Cycle Time	Successful Packets	PDR
<b>No Retransmissions; No Frequency/Channel Hopping</b>				
Single-hop	7213	30 timeslots (15 ms)	209173	99.9%
<b>Schedule Duplication without Frequency/Channel Hopping</b>				
Single-hop	7229	60 timeslots (30 ms)	209641	100%

### D. Technology Demonstrations

We have demonstrated the basic concept of GALLOP and its viability for handling versatile closed-loop control applications with fast dynamics. In [37], we have demonstrated GALLOP for remote control and formation control of mobile platforms. In [38], we have demonstrated the scenario of remotely balancing a two-wheeled robot over GALLOP that represents an inverted pendulum on wheels.

## VIII. CONCLUDING REMARKS

Realizing wireless closed-loop control is crucial for mission-critical IIoT systems. This paper presented GALLOP, which has been designed to provide high-performance connectivity for achieving wireless closed-loop control over multi-hop networks. GALLOP implements novel control-aware multi-hop scheduling for handling bi-directional cyclic information exchange and retransmission techniques that leverage cooperative transmissions for successful operation in harsh wireless environments. Performance evaluation through hardware implementation on a Bluetooth 5 platform and extensive system-level simulations demonstrate that GALLOP provides highly scalable connectivity with very low and deterministic latency and very high reliability. The results also demonstrate the viability of handling control loops with fast dynamics (on the order of few ms), rapid convergence and single-hop operation. GALLOP can be extended to a broad range of legacy and emerging IIoT applications.

GALLOP is one of the first protocols designed for wireless closed-loop control. There are a number of avenues for further work in terms of protocol enhancements, implementation and application design. From protocol perspective, some of the key directions for future work include MAC layer reconfigurability for dynamic adaptation of scheduling parameters, operation of multiple single-hop networks, enhancements for wireless closed-loop control with node mobility, and integration of antenna diversity techniques. From implementation perspective, it is important to realize GALLOP over a Wi-Fi radio for achieving high-speed and high-performance connectivity for multimedia-centric industrial control applications. The high-performance connectivity offered by GALLOP opens up various new possibilities for *communication-oriented* design of robotics-centric applications (e.g., formation control of mobile platforms), as opposed to conventional control-oriented designs which leverage complex sensory capabilities and architectures. Therefore, an important area of future work is exploitation of GALLOP in cooperative robotics applications, especially from the perspective of control-wireless co-design.

## REFERENCES

- [1] A. Aijaz, A. Stanoev, and U. Raza, "GALLOP: Toward High-performance Connectivity for Closing Control Loops over Multi-hop Wireless Networks," in *ACM International Conference on Real-Time Networks and Systems (RTNS)*, 2019, pp. 176–186.
- [2] Y. Liao, E. de Freitas Rocha Loures, and F. Deschamps, "Industrial Internet of Things: A Systematic Literature Review and Insights," *IEEE Internet Things J.*, vol. 6, no. 6, pp. 4515–4525, Dec. 2018.
- [3] E. Sisinni *et al.*, "Industrial Internet of Things: Challenges, Opportunities, and Directions," *IEEE Trans. Ind. Informat.*, vol. 14, no. 11, pp. 4724–4734, Nov 2018.



- [4] J.-Q. Li *et al.*, “Industrial Internet: A Survey on the Enabling Technologies, Applications, and Challenges,” *IEEE Commun. Surveys Tuts.*, vol. 19, no. 3, pp. 1504–1526, Third Quarter 2017.
- [5] Z. Ma *et al.*, “High-Reliability and Low-Latency Wireless Communication for Internet of Things: Challenges, Fundamentals, and Enabling Technologies,” *IEEE Internet Things J.*, vol. 6, no. 5, pp. 7946–7970, 2019.
- [6] J.-D. Decotignie, “Ethernet-Based Real-Time and Industrial Communications,” *Proc. IEEE*, vol. 93, no. 6, pp. 1102–1117, June 2005.
- [7] A. Aijaz and M. Sooriyabandara, “The Tactile Internet for Industries: A Review,” *Proc. IEEE*, vol. 107, no. 2, pp. 414–435, 2018.
- [8] G. Scheible, D. Dzung, J. Endresen, and J. E. Frey, “Unplugged but Connected [Design and Implementation of a Truly Wireless Real-time Sensor/Actuator Interface],” *IEEE Ind. Electron. Mag.*, vol. 1, no. 2, pp. 25–34, Summer 2007.
- [9] PNO, “WSAN Air Interface Specification,” 2012. [Online]. Available: <http://www.profibus.com/nc/download/installation-guide/downloads/wsan-air-interface-specification/display/>
- [10] IO-Link Community, “IO-Link Wireless System Extensions,” IO-Link, Specification 10.112, March 2018. [Online]. Available: [https://io-link.com/share/Downloads/System-Extensions/IO-Link\\_Wireless\\_System\\_10112\\_V11\\_Mar18.pdf](https://io-link.com/share/Downloads/System-Extensions/IO-Link_Wireless_System_10112_V11_Mar18.pdf)
- [11] A. Aijaz, “ENCLOSE: An Enhanced Wireless Interface for Communication in Factory Automation Networks,” *IEEE Trans. Ind. Informat.*, vol. 14, no. 12, pp. 5346–5358, Dec 2018.
- [12] “Siemens SCALANCE W,” <http://w3.siemens.com/mcms/industrial-communication/en/industrial-wireless-communication/iwlan-industrial-wireless-lan/pages/iwlan.aspx>, accessed: 2017-10-15.
- [13] IEC, “Industrial Networks – Wireless Communication Network and Communication Profiles – WIA-FA,” International Electrotechnical Commission (IEC), Standard 62948, 2017. [Online]. Available: <https://webstore.iec.ch/publication/32718>
- [14] A. Aijaz, “High-Performance Industrial Wireless: Achieving Reliable and Deterministic Connectivity over IEEE 802.11 WLANs,” *IEEE Open Journal of the Industrial Electronics Society*, 2020. [Online]. Available: <https://arxiv.org/abs/2003.10188>
- [15] C. Dombrowski and J. Gross, “EchoRing: A Low-Latency, Reliable Token-Passing MAC Protocol for Wireless Industrial Networks,” in *European Wireless (EW) Conf.*, May 2015, pp. 1–8.
- [16] B. Hofeld *et al.*, “Wireless Communication for Factory Automation: An Opportunity for LTE and 5G Systems,” *IEEE Commun. Mag.*, vol. 54, no. 6, pp. 36–43, June 2016.
- [17] A. Aijaz, “Private 5G: The Future of Industrial Wireless,” *IEEE Ind. Electron. Mag.*, vol. 14, no. 4, pp. 136–145, 2020.
- [18] R. Alur *et al.*, “Compositional Modeling and Analysis of Multi-Hop Control Networks,” *IEEE Trans. Autom. Control*, vol. 56, no. 10, October 2011.
- [19] F. Smarra, A. D’Innocenzo, and M. D. D. Benedetto, “Optimal Co-design of Control, Scheduling and Routing in Multi-hop Control Networks,” in *IEEE Conf. on Decision and Control (CDC)*, Dec. 2012, pp. 1960–1965.
- [20] M. Pajic, S. Sundaram, G. Pappas, and R. Mangharam, “The Wireless Control Network: A New Approach for Control Over Networks,” *IEEE Trans. Autom. Control*, vol. 56, no. 10, pp. 2305–2318, Oct. 2011.
- [21] S. Tatikonda and S. Mitter, “Control under Communication Constraints,” *IEEE Trans. Autom. Control*, vol. 49, no. 7, pp. 1056–1068, July 2004.
- [22] C. L. Robinson and P. R. Kumar, “Optimizing Controller Location in Networked Control Systems with Packet Drops,” *IEEE J. Sel. Areas Commun.*, vol. 26, no. 4, pp. 661–671, May 2008.
- [23] L. Zhang, H. Gao, and O. Kaynak, “Network-Induced Constraints in Networked Control Systems – A Survey,” *IEEE Trans. on Ind. Informat.*, vol. 9, no. 1, pp. 403–416, Feb 2013.
- [24] A. Sgora, D. J. Vergados, and D. D. Vergados, “A Survey of TDMA Scheduling Schemes in Wireless Multihop Networks,” *ACM Comput. Surv.*, vol. 47, no. 3, pp. 1–39, 2015.
- [25] X. X. Teh, A. Aijaz, A. Portelli, and S. Jones, “Communications-Based Formation Control of Mobile Robots: Modeling, Analysis and Performance Evaluation,” in *ACM Intl. Conf. on Modeling, Analysis and Simulation of Wireless and Mobile Systems (MSWiM)*, 2020, p. 149–153.
- [27] F. Ferrari, M. Zimmerling, L. Thiele, and O. Saukh, “Efficient Network Flooding and Time Synchronization with Glossy,” in *ACM/IEEE Intl. Conf. on Information Processing in Sensor Networks (IPSN)*, April 2011, pp. 73–84.
- [26] T. Winter, “IPv6 Routing Protocol for Low Power and Lossy Networks,” RFC 6550, Mar. 2012. [Online]. Available: <https://rfc-editor.org/rfc/rfc6550.txt>
- [28] T. Chang, T. Watteyne, X. Vilajosana, and P. H. Gomes, “Constructive Interference in 802.15.4: A Tutorial,” *IEEE Commun. Surveys Tuts.*, vol. PP, no. 99, Sept. 2018.
- [29] M. Zimmerling, L. Mottola, and S. Santini, “Synchronous Transmissions in Low-Power Wireless: A Survey of Communication Protocols and Network Services,” 2020. [Online]. Available: <https://arxiv.org/abs/2001.08557>
- [30] M. Iezzi, M. D. Renzo, and F. Graziosi, “Closed-Form Error Probability of Network-Coded Cooperative Wireless Networks with Channel-Aware Detectors,” in *IEEE Global Telecommun. Conf. (GLOBECOM)*, Dec 2011, pp. 1–6.
- [31] S. C. Liew, S. Zhang, and L. Lu, “Physical-layer Network Coding: Tutorial, Survey, and Beyond,” *Physical Commun.*, vol. 6, pp. 4 – 42, 2013.
- [32] Z. Khalid and S. Durrani, “Distance Distributions in Regular Polygons,” *IEEE Trans. Veh. Technol.*, vol. 62, no. 5, pp. 2363–2368, Jun 2013.
- [33] A. Dimakis and J. Walrand, “Sufficient Conditions for Stability of Longest-Queue-First Scheduling: Second-Order Properties using Fluid Limits,” *Adv. Appl. Probab.*, vol. 38, no. 2, p. 505–521, 2006.
- [34] R. Lim, R. Da Forno, F. Sutton, and L. Thiele, “Competition: Robust Flooding Using Back-to-Back Synchronous Transmissions with Channel-Hopping,” in *International Conference on Embedded Wireless Systems and Networks (EWSN)*, USA, 2017, p. 270–271.
- [35] M. Baddeley *et al.*, “Atomic-SDN: Is Synchronous Flooding the Solution to Software-Defined Networking in IoT?” *IEEE Access*, vol. 7, pp. 96 019–96 034, 2019.
- [36] Bluetooth SIG, “Mesh Profile,” Specification v1.0, 2017. [Online]. Available: <https://www.bluetooth.com/specifications/mesh-specifications>
- [37] A. Aijaz, A. Stanoev, and M. Sooriyabandara, “Toward Real-Time Wireless Control of Mobile Platforms for Future Industrial Systems,” in *IEEE Intl. Conf. on Computer Communications (INFOCOM)*, April 2019. [Online]. Available: <https://arxiv.org/abs/1907.01979>
- [38] A. Stanoev, A. Aijaz, A. Portelli, and M. Baddeley, “Demo: Closed-Loop Control over Wireless - Remotely Balancing an Inverted Pendulum on Wheels,” in *ACM Intl. Conf. on Embedded Wireless Systems and Networks (EWSN)*, Feb. 2020, pp. 195–197.



**Adnan Aijaz** (M’14–SM’18) studied telecommunications engineering at King’s College London, United Kingdom, where he received a Ph.D. degree in 2014 for research in wireless networks. He joined the Bristol Research and Innovation Laboratory (formerly Telecommunications Research Laboratory) of Toshiba Corporation in 2015, where he currently holds the position of Innovation Programme Lead. His recent research areas include industrial communication systems and automation networks, cyber-physical systems, next generation Wi-Fi and cellular (5G and beyond) technologies, and robotics and autonomous systems. He has been contributing to various national and international research projects and standardization activities related to industrial communication.



**Aleksandar Stanoev** received the M.Eng. degree (Hons.) from the University of Bristol, United Kingdom, in 2018. He is currently a Senior Research Engineer with the Bristol Research and Innovation Laboratory of Toshiba Corporation. His current research interests include low-power wireless MAC protocols, large-scale smart city deployments and their design challenges, and embedded IoT hardware design. He is also a Maintainer of the Contiki-NG open-source IoT operating system.